Astron. Astrophys. 235, 22–34 (1990)

ASTRONOMY
AND
ASTROPHYSICS

Stellar population analysis of the red and blue galaxies in the distant cluster Abell 370

P. Jablonka[1], D. Alloin[1], and E. Bica[2]

[1] Observatoire de Paris, DAEC, URA 173 CNRS, F-92195 Meudon Principal Cédex, France
[2] Universidade Federal do Rio Grande do Sul, Departamento de Astronomia,
Av. Bento Gonçalves, 9500, 91500 Porto Alegre-RS, Brazil

Received August 18, accepted December 27, 1989

Abstract. In this paper, we apply a population synthesis method based on star cluster integrated spectral properties to members of the distant galaxy cluster Abell 370. Within boxes defined from magnitude vs colour diagrams, we have co-added the data corresponding to members with similar spectral characteristics, in order to achieve a signal to noise ratio suitable for the synthesis.

Population synthesis of the two blue averaged objects provides the flux and mass fractions of the young components responsible for their blue colours. These are the disc component in late spiral galaxies for one group and a recent starburst for the other group.

Population synthesis of the three red averaged objects confirms that no cosmological evolutionary effects are observed in this cluster at $z=0.374$. In all three cases, we find a metallicity enrichment lower than that expected on the basis of the metallicity vs luminosity relationship found for the central regions of nearby galaxies. For the less luminous objects, which correspond to present-day massive elliptical galaxies, this reflects the contamination by light from their metal-poor halo population, as a result of Abell 370 distance. For the more luminous objects, which correspond rather to cD and extremely massive galaxies, their low metallic content implies that they were formed through merging processes occurring once the acting galaxies had already achieved the bulk of their star formation process and chemical evolution.

Key words: cosmology – clusters: of galaxies – galaxies: stellar content of – galaxies: evolution of – spectroscopy

1. Introduction

Observing high redshift galaxies allows one to directly look back in time, and hence, possibly track some cosmological evolution of the galaxy populations. If the universe is probed far enough, one may hope to reach the redshift slice where intense star formation occurred in the body of giant galaxies and, from this, constrain the epoch of galaxy formation.

Over the past decade, a few galaxy spectra at lookback ages down to 3 Gyr ($z\sim4$) have been collected, thanks to larger telescopes and more sensitive detectors (e.g. Gunn and Dressler, 1988 and references therein). However, it is still easier to access galaxy clusters in the redshift range 0.3 to 0.4, corresponding to lookback ages around 11 Gyr, and to study their stellar content from spectroscopic data with suitable signal to noise ratio. They do contain red members with spectral properties similar to those encountered in nearby giant elliptical galaxies (Couch and Sharples, 1987; Pickles and van der Kruit, 1988; Persson, 1988; O'Connell, 1988). This suggests that major evolutionary effects of cosmological nature do not yet show up at redshift 0.4. It also implies that the epoch at which the bulk of stars were formed in these galaxies goes well back into the past.

Although most galaxy clusters observed so far with redshift up to 0.9 exhibit red members like their present-day counterparts, there seems to be a trend for distant clusters to show an excess of blue galaxies (Butcher and Oemler, 1978). This was first suggested from photometric studies and, more recently, has been supported by spectroscopic data (Dressler and Gunn, 1982; Butcher and Oemler, 1984; Sharples et al., 1985). The reality of this effect has been questioned however, on the basis of selection effects in the cluster sample (Koo, 1988). And indeed, blue galaxy excesses might not be restricted to compact cluster cores and might pertain to a more general phenomenon, also showing up in the field population (Ellis, 1988).

In the light of previous studies which presented Abell 370 as a rich galaxy cluster, at $z=0.374$, with a substantial fraction of blue objects, we aim at *analyzing in a quantitative way* the composite stellar populations of its red and blue galaxies. Early analyses have been performed through both photometric and spectroscopic techniques (Bautz et al., 1982; Butcher and Oemler, 1984; Henry and Lavery, 1987; McLaren et al., 1987; Mellier et al., 1988). Stellar population analyses for Abell 370, as for distant galaxy clusters in general, have only been performed so far through comparisons between observations and predetermined models, or templates of global galaxies: the intention was more often to so derive the cluster galaxy morphological types. For Abell 370, Mellier et al. (1988) have compared individual galaxy spectra with synthetic ones from Rocca-Volmerange and Guiderdoni (1988); while McLaren et al. (1987) have confronted their multiple band photometry to the spectral energy distributions from nearby galaxies of various morphological types (Pence, 1979; Coleman et al., 1980). For a direct analysis of composite stellar populations, one requires however high signal-

Send offprint requests to: P. Jablonka

to-noise data. Therefore, Pickles and van der Kruit (1988) have synthesized the brightest red member of Abell 370 only, using a stellar library: they concluded that most stars in this object formed well before the lookback time corresponding to redshift 0.374.

Proceeding with stellar population synthesis and looking for cosmological evolutionary effects in distant galaxy clusters, *it is imperative to take into account metallicity effects, in addition to age*. With that goal, we have recently developed a new population synthesis method which uses a library of star cluster integrated spectra and a grid of their spectral properties extrapolated to appropriate metallicities (Bica and Alloin, 1988 and references therein). Through a study of a large sample of galaxy nuclei, this approach has already proved to be quite powerful at deriving the star formation history and the overall chemical enrichment in composite populations (Bica, 1988; Bica et al., 1988). We derive the flux contributions from successive {age, metallicity} components and transform them into mass fractions. In a subsequent step, we discuss their possible interpretation in terms of bulges, spiral discs, starbursts or galaxy mergers.

We present in Sect. 2 the cluster galaxy data base and our co-adding criteria, having to group objects for signal-to-noise ratio improvement. Once the groups have been defined, we provide in Sect. 3 a brief comparison of their average spectra with those of the central regions in nearby typical galaxies, then we present and discuss the results of our population syntheses. Concluding remarks are given in Sect. 4.

2. Spectroscopic data and group definition

We have used the spectroscopic catalogue of galaxies in the direction of Abell 370 cluster (Soucail et al., 1988, hereafter SMFC). It consists of multispectroscopic observations, in the 4500 to 7500 Å range, through the PUMA system at the CFH and ESO 3.6 m telescopes. Details on the observing and reduction procedures are given in SMFC. Of the 84 spectra in the catalogue, we have restricted our attention to those with $0.36 < z < 0.39$, which we consider as pertaining to galaxy members of Abell 370. From this subsample we have selected spectra with a reasonable signal-to-noise ratio: our lower threshold corresponds to the signal-to-noise ratio achieved for galaxies nos. 45, 47, 54 and 87 in SMFC. We adopt in our study the designation numbers labelled "CCD" in SMFC; whenever necessary, we also use the BOW designations (Butcher et al., 1983). We end up with 29 spectra to be studied below. Each has been rebinned to restframe, according to its redshift value z listed in SMFC. The restframe spectral range corresponds to 3100 Å $< \lambda <$ 5600 Å. It should be noticed that for the redshift-corrected spectra, spectral regions around 4050 and 5000 Å are disturbed by residuals of the 5577 Å night sky emission and of the B band absorption of O_2 at 6870 Å, respectively, and that, for $\lambda > 5250$ Å, the data precision decreases owing to residuals of night sky OH emission.

In order to perform a population synthesis, a much higher signal-to-noise ratio is required than that available for most spectra of individual galaxies in the catalogue. Consequently, we have co-added spectra according to the following criteria:

(i) We have delineated boxes in colour vs magnitude diagrams derived from the R 24.5 and B 26.5 photometry in SMFC and from the J and N photometry in Butcher et al. (1983). These diagrams are shown in Figs. 1a and 1b respectively. The galaxies defining each of the groups occupy essentially the same loci in these two independent diagrams, although the SMFC diagram appears to be slightly more scattered. Basically, these boxes prevent co-addition of similar spectra from objects differing by more than one magnitude in B or N. Final box contours were delineated according to a joint consideration of the two diagrams. The photometric colours isolate red groups (R1 through R3) from blue ones (B1 and B2).

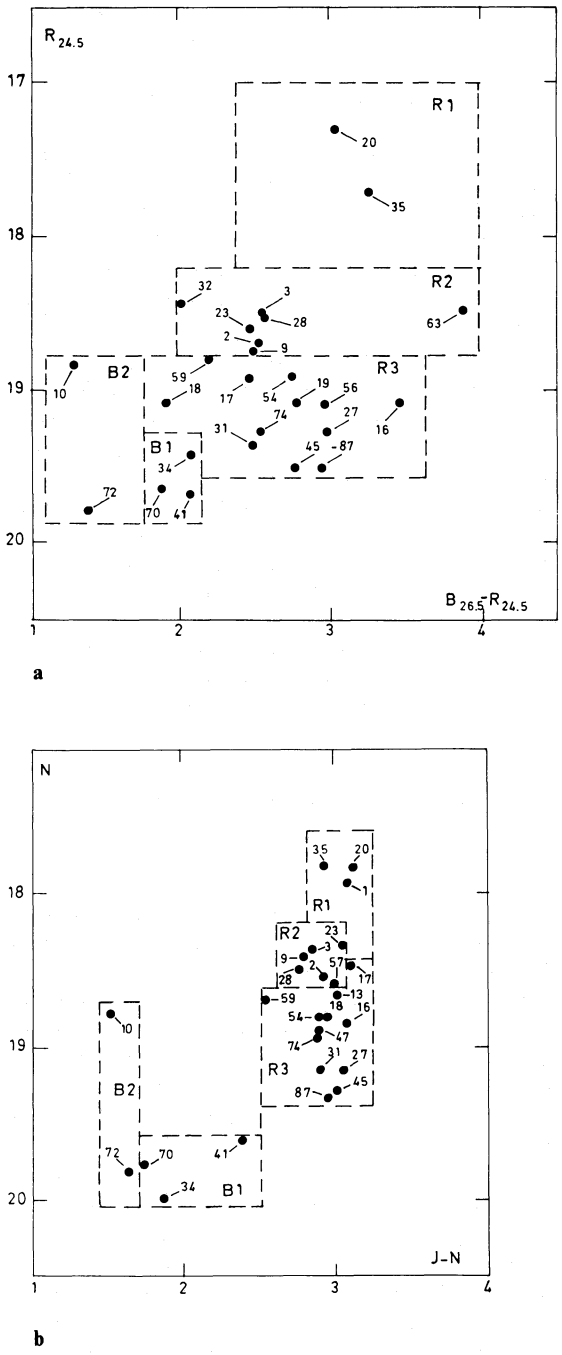

a

b

Fig. 1. a the colour ($B-R$), magnitude (R) diagram, data from SMFC. Galaxies with numbers 1, 47 and 57 do not have data corresponding to this plot. **b** the colour ($J-N$), magnitude (N) diagram, data from Butcher et al. (1983). Galaxies with numbers 32, 56, 63 and 76 have no data to be plotted in this daigram

(ii) Spectra which are essentially identical in terms of continuum distribution and absorption features as long as these are discernible.

(iii) Before co-adding spectra within each group, we assigned them weights, according to their signal-to-noise ratio.

The members of each group are listed in Table 1, where we compare also their morphological type identification as derived by SMFC and McLaren et al. (1987). After these authors, the red groups contain mostly galaxies classified as E/S0 or early type spirals; while the blue groups are claimed to be built of late type spirals and irregulars. It is worth pointing out that the agreement between SMFC and McLaren et al. classifications is good, although such a classification is a difficult exercise, owing to the limited signal-to-noise ratio of individual spectra and to the lack of spectral resolution in the case of broad-band photometric data. For example, integrated models (Rocca-Volmerange and Guiderdoni, 1988) and templates (Pence, 1979; Coleman et al., 1980) do not predict large significant differences between E/S0 galaxies and early type spirals, across the narrow wavelength range covered by SMFC and McLaren et al. observations.

We conclude that our co-adding criteria have allowed a compromise to be reached between the obtention of average spectra appropriate for population synthesis and the prohibitive addition of spectra differing too much. We now proceed with the population synthesis of the representative of each group.

3. Population analysis of the representative galaxy groups in Abell 370

3.1. Representative spectra of the galaxy groups

The average spectra for the red groups R1 through R3 and the two blue groups B1 and B2, a result of the co-adding procedure just described, are displayed in Fig. 2a. For a qualitative comparison, we show in Fig. 2b a selection of template spectra from a sample of nearby galaxies (Bica, 1988). Let us stress the fact that galaxies in Abell 370, because of their small angular diameter, are almost seen globally through the apertures of the PUMA mask; instead nearby galaxy spectra refer to their central regions, 1 kpc diameter across.

Red groups in Abell 370 exhibit spectra which have counterparts among the nearby galaxy templates. However none of the R1 to R3 groups appears to be as red and strong-lined as template E1 (Fig. 2b) which stands for the central region of massive elliptical galaxies. This is not surprising as, at the Abell 370 distance and with the apertures used for the observations, the light from the metal-rich central populations of a massive elliptical galaxy will be mixed with its halo metal-poor contribution. Conversely, we expect that late spiral galaxies, seen globally at the distance of Abell 370, would exhibit bluer composite spectra because of their disc component: this is neither the case for groups R1 to R3.

Average spectra for the blue groups B1 and B2 show that an important hot stellar component is present, responsible for the strong Hε through Hγ Balmer absorption series, as well as the [O II] and [O III] emission lines. The question is to know whether these blue components correspond to the disc population of a late spiral galaxy, to the population I contribution from an irregular or to a more exceptional burst of star formation. A few examples of comparable situations in the central region of nearby galaxies are displayed in Fig. 2b. A direct comparison in Fig. 2 of groups B1 and B2 to the nearby cases of blue nuclei S6 and E8, shows that an explanation in terms of a starburst is possible at first sight. We think however that a quantitative population analysis as presented below is required in order to bring a more precise answer.

Table 1. Galaxy members for each group in Abell 370. "BOW" refers to the numbering in Butcher et al. (1983) "CCD" refers to the numbering in Soucail et al. (1988), hereafter SMFC

Designation number		Morphological type	
"BOW"	"CCD" SMFC	SMFC (1988)	McLaren et al. (1987)
R1			
14	1	Sb	—
10	20	E	E/S0
9	35	E	E/S0
R2			
31	2	E	—
22	3	E	—
24	9	Sa/E	E/S0
21	23	E	E/S0
29	28	Sa	E/S0+UV
—	32	E	—
32	57	Sb	—
—	63	Sb	—
R3			
34	13	E	E/S0
45	16	?	E/S0
26	17	E	E/S0
41	18	E	E/S0
63	27	E	E/S0
62	31	Sa	—
75	45	Sc	—
50	47	E	—
43	54	Sa	E/S0
—	56	E	—
36	59	Sb	—
55	74	E	E/S0
80	87	E	E/S0
B1			
165	34	Sc/Sd	Scd
108	41	Sc	—
128	70	Irr	Scd
B2			
39	10	Irr	Scd
137	72	Irr	—

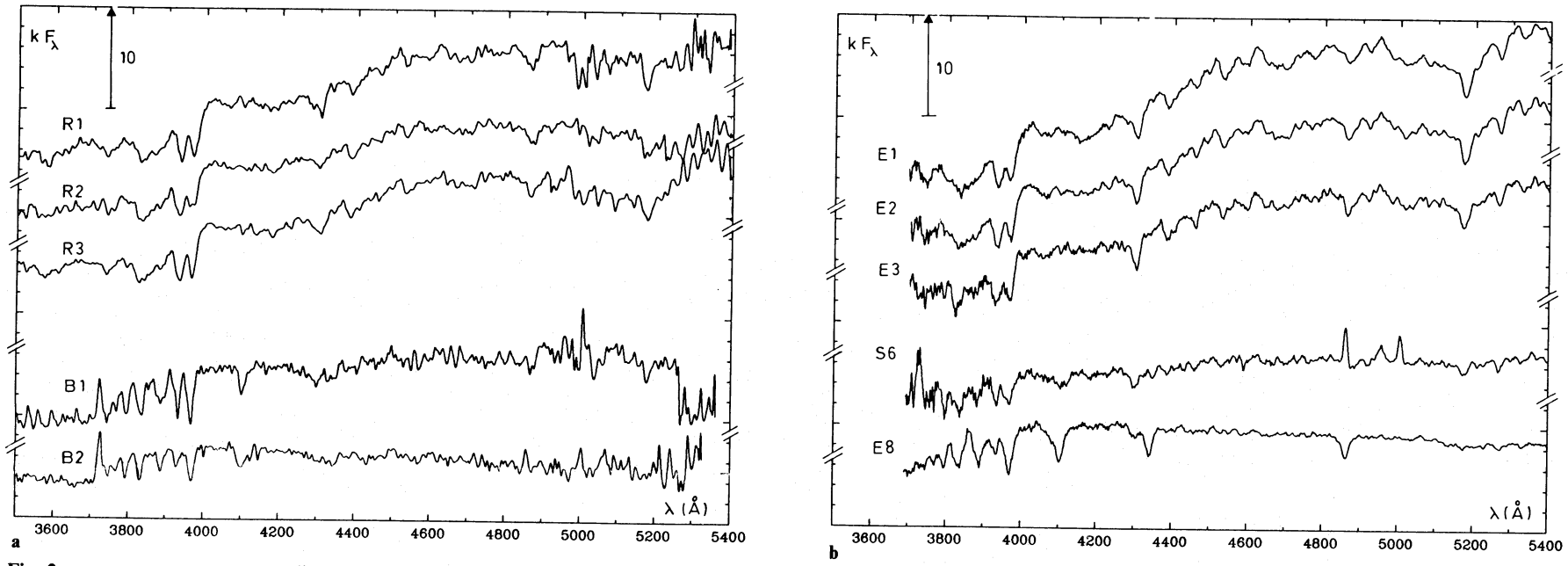

Fig. 2. **a** average spectra corresponding to the identified groups in Abell 370: red groups R1 to R3, blue groups B1 and B2; **b** nearby templates for galaxy central regions from Bica (1988): elliptical and S0 galaxies are denoted E, spiral galaxies S. After Bica (1988) template S6 consists of a weak star forming event younger than 10^8 yr, superimposed on an old component. Template E8 represents a strong star formation burst, 5 10^8 yr old, on top of an old metal deficient population

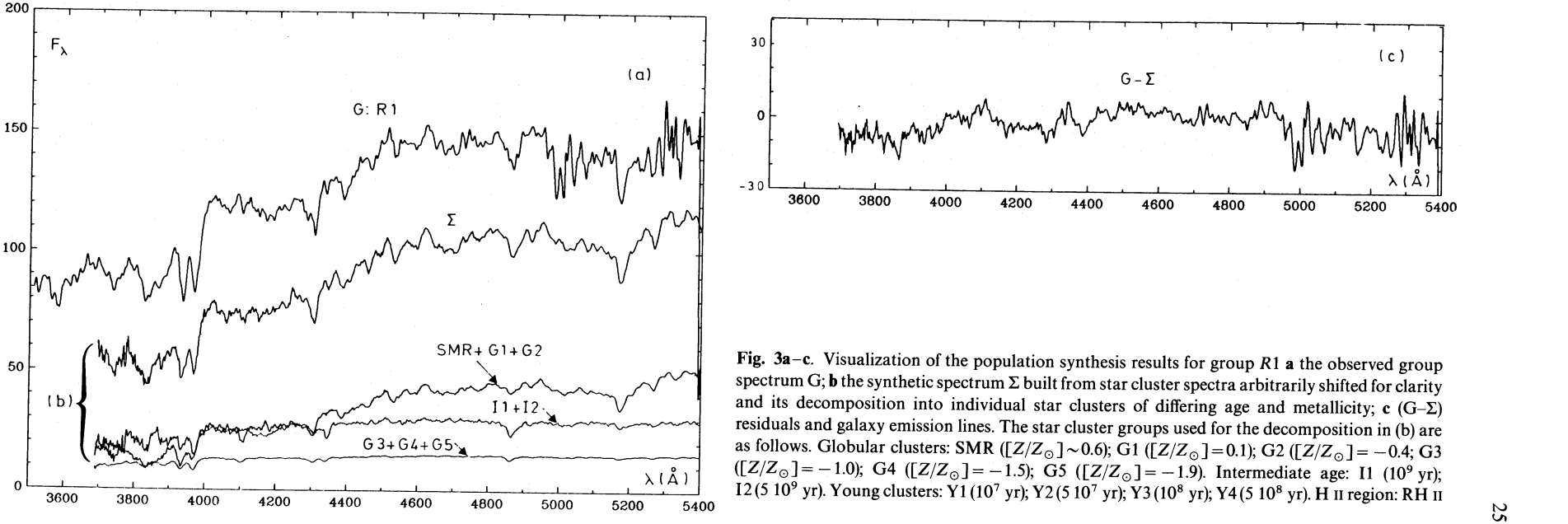

Fig. 3a–c. Visualization of the population synthesis results for group *R1* **a** the observed group spectrum G; **b** the synthetic spectrum Σ built from star cluster spectra arbitrarily shifted for clarity and its decomposition into individual star clusters of differing age and metallicity; **c** (G–Σ) residuals and galaxy emission lines. The star cluster groups used for the decomposition in (b) are as follows. Globular clusters: SMR ($[Z/Z_\odot] \sim 0.6$); G1 ($[Z/Z_\odot] = 0.1$); G2 ($[Z/Z_\odot] = -0.4$; G3 ($[Z/Z_\odot] = -1.0$); G4 ($[Z/Z_\odot] = -1.5$); G5 ($[Z/Z_\odot] = -1.9$). Intermediate age: I1 (10^9 yr); I2 (5 10^9 yr). Young clusters: Y1 (10^7 yr); Y2 (5 10^7 yr); Y3 (10^8 yr); Y4 (5 10^8 yr). H II region: RH II

3.2. Population synthesis of the representative galaxy groups in Abell 370

3.2.1. Some remarks about the population synthesis method

The population synthesis method we apply has been largely described in Bica (1988). It makes use of a base of star cluster integrated spectra from which *a grid of star cluster spectral properties has been built as a function of age and metallicity*. Then, the spectral properties from composite systems are reproduced through combinations of elements appearing in the grid. The results are expressed in terms of the percentage flux contribution at 5870 Å, from the relevant cluster grid elements. The restricted number of parameters to consider – age and metallicity – and the use of fast computers allow one to test a fairly large number of combinations, thus to be more confident about the uniqueness of the encountered solution (Bica, 1988). Besides, we use chemical evolution arguments to restrict the region in the metallicity vs age plane where solutions will be searched for. We combine the appropriate number of grid clusters, in relation with the chemical evolutionary path we test and with the opportunity we have to cover an age range from H II regions to old globular clusters and a metallicity range $[Z/Z_\odot]$ from -2 to $+0.6$. As we lack time resolution for ages older than 8 Gyr (globular clusters), we cannot follow the early chemical enrichment in galaxies. Thus, in practice, the evolutionary path is essentially made of two sequences: (1) a metallicity sequence from $[Z/Z_\odot]=-2$ to $[Z/Z_\odot]_{max}$ within the old age bin and (ii) an age sequence down to 10^6 yr at constant $[Z/Z_\odot]_{max}$. Then, we test the relative contributions of the different types of grid clusters along the path, varying them by steps between 5 and 20%. In the case of Abell 370, this process resulted in the use of about 12 clusters and of a 10% step. The algorithm selects all the combinations which allow one to reproduce the spectral properties of the composite system, spectral feature equivalent widths W_λ, within their respective error-bars, the values of which depend on the signal-to-noise ratio of the data to be matched. We find in general a set of degenerate, close-by solutions forming a family. The number of possible solutions with respect to the total number of tested combinations is around 10^{-3} in the present study.

In this analysis we had to face some limiting factors. First, the data cover a restricted wavelength range 3500 to 5400 Å. One should remember that this spectral domain is not the best suited for disentangling age from metallicity effect (Schmidt et al., 1989). Second, the region redwards of 5000 Å is polluted by residuals from night sky lines and bands, so that we had to consider the Mg I, MgH blend with a particular attention: we chose to attach to this feature an enlarged window, so that its weight should be low in the computation (this was particularly critical for groups R3 and B1). In the blue groups, where the Hβ line was obviously contaminated by some emission component, we used a similar procedure. Finally, comparison between the synthetic spectrum Σ resulting from the population analysis, as visualized with the base star cluster spectra, and the observed spectrum G allows us to evaluate the average intrinsic reddening $E(B-V)$ for each group. Twelve base star clusters are available for visualization of the composite population computed from the grid star clusters, with ages from 10^6 to 1.65×10^{10} yr. The metallicity of the most metallic clusters in our base (group G1 in Fig. 3) is solar, or perhaps slightly above solar, as this group includes clusters towards the bulge of our Galaxy, NGC 6528 and 6553. Besides, we have used the predicted spectrum of a globular cluster at $[Z/Z_\odot]=0.6$, super metal-rich SMR, derived from the population analysis of giant elliptical and S0 galaxies (Bica, 1988). This base of available spectra is quite suitable for the visualization of computed composite populations in the present study (see Sect. 2.2).

3.2.2. Results of the population analysis for the red groups R1 through R3

Let us remind that the actual input from the representative galaxy groups for the synthesis are the observed equivalent widths W_λ of seven spectral features (bottom part of Table 2). We check for an eventual intrinsic reddening $E(B-V)$ by scaling the observed galaxy continuum to the synthetic one.

We present in Table 2, for the three groups, the population synthesis results. It should be emphasized that, owing to the limited spectral range available, we have not looked for complex, unconstrained solutions, restricting our search to the first order scenarios related to chemical evolutionary paths. The fit can be tested through the residue values, $W_{\lambda,\,obs}-W_{\lambda,\,syn}$, and their comparison with the quoted error-bars on $W_{\lambda,\,obs}$ (Table 2, Test). Visulizations of the synthesis results are shown in Figs. 3 through 5. Display of the results for groups R1 to R3 should not be too much affected by the limitation described in Sect. 2.1. Indeed, they exhibit comparable flux contributions from the old and from the $5\,10^9$ yr age bins at metallicity $[Z/Z_\odot]=0.3$. Although we do not have available cluster spectra at this metallicity, we have used for the former the SMR globular cluster spectrum at $[Z/Z_\odot]=0.6$ and, for the later, a star cluster of intermediate age and $[Z/Z_\odot]=-0.4$. As a mean, the components at $[Z/Z_\odot]=0.3$ revealed in the synthesis, should be satisfactorily represented. Visualization for group R2 can be thoroughly achieved with the available cluster spectra. By comparing the synthetic continuum to the observed one, obtained figures for the intrinsic reddening $E(B-V)$ are between 0.05 and 0.1 for group R1 through R3, very close to the one encountered in the central regions of nearby elliptical galaxies, $E(B-V)\sim0.04$ (Bica, 1988).

We have then transformed the percentage flux contribution from each stellar generation (grid element) into a mass contribution. This has been performed by means of theoretical M/L_v ratios for single generation stellar systems computed at different ages (Bica et al., 1988). The results are displayed in Fig. 6.

We did the objects grouping blindly with respect to the morphological types previously attributed to them. Yet, from the analysis by Soucail et al. (1988), some early spiral galaxies should be present in our red groups. However, the synthesis results do not provide evidence for the presence of a disc component in any of the red groups in Abell 370. From the present analysis, groups R1 through R3 appear to be dominated by old, metal-rich populations, just like in present-day massive elliptical galaxies; hence, we do not find any cosmological evolutionary effect in Abell 370, at $z=0.374$.

Let us now discuss each group in detail. As noticed in a previous work (Bica and Alloin, 1987), when the contribution from young components is negligible, a sensitive metallicity indicator is the combined equivalent width W(CN 4150, 4214) $+W$(Mg I + MgH, 5156, 5196) which increases with the total absolute luminosity of the galaxy. We can place in the corresponding plot for the central regions in nearby galaxies (Fig. 7), groups R1 through R3, using the N magnitude from Butcher et al. (1983). We observe that all three red groups in Abell 370 fall apart

Table 2. Percentage flux contributions at 5870 Å from the different {age, metallicity} components in the composite stellar populations of groups R1, R2 and R3 in Abell 370. The intrinsic reddening value $E(B-V)$ is also indicated. In the part of the table labelled Test, we provide the observed equivalent width of the features used for the synthesis, as well as the residues ($W_{\lambda,\,obs} - W_{\lambda,\,syn}$) for each model. The residue is sometimes larger than the error-bar on the measurement as it relates more directly to the "window" assigned in the computation to each spectral feature, equal to or larger than the measurement error

H II 10^7	$5\,10^7$	10^8	$5\,10^8$	10^9	$5\,10^9$	Old	Age $[Z/Z_\odot]$	
				4.5	26	22.5	+0.3	
						19.5	0	
$\{E(B-V)\sim 0.1\}$						12	−0.5	R1
						7.5	−1	
						5	−1.5	
						3	−2	
				1	18	33	0	
						29	−0.5	
$\{E(B-V)\sim 0.05\}$						12	−1	R2
						5	−1.5	
						2	−2	
			2	9.5	24	19	+0.3	
						18	0	
$\{E(B-V)\sim 0.05\}$						12	−0.5	R3
						8	−1	
						5	−1.5	
						2.5	−2	

Test features	Observed W_λ(Å); residue		
	R1	R2	R3
Ca II K	16.7±0.4; +0.9	16.0±0.4; +1.7	16.5±0.3; +1.2
Hδ	3.4±0.6; −0.3	4.1±0.5; −0.9	4.3±0.2; −0.9
CN 4216	11.9±0.9; +1.0	8.9±0.7; +0.2	11.5±0.3; +0.8
CH Gband	9.1±0.5; +0.5	5.8±0.4; −2.0	8.1±0.2; −0.2
Hγ	5.9±0.8; +0.6	4.2±0.6; −0.9	5.0±0.3; −0.6
Hβ	3.8±0.9; −1.5	2.9±1.2; −0.5	3.5±1.0; −1.3
Mg I+MgH	8.0±1.0; +0.9	6.6±1.1; +0.7	9.3±2.3;

from this relationship, exhibiting too low a metallicity index for their absolute luminosity. The population synthesis results show the same tendency (Table 2). We find that the maximum metallicity achieved in groups R1 and R3 is $[Z/Z_\odot]\sim 0.3$, while in group R2, it is about solar.

Remember that the metallicity index measured in the spectra for E1 through E4 relates to the population contained within a 1 kpc diameter region. That measured in Abell 370 galaxy groups relates to a much larger region within the galaxy (around 20 kpc). The position of group R3 in Fig. 7 can then be easily understood: although it shows an absolute luminosity comparable to that of present-day massive elliptical galaxies, its weak value of $W(\mathrm{CN})+W(\mathrm{Mg\,I}+\mathrm{Mg\,H})$, reflected in the population synthesis result $[Z/Z_\odot]_{max}=0.3$ only, is most likely due to light *dilution by a metal-poor halo component*. The corresponding metallicity lowering is of around 0.3 dex.

In contrast, both groups R1 and R2 exhibit an absolute luminosity which exceeds that of massive elliptical galaxies. Group R2 displays much lower a metallicity index than the one we would have expected on the basis of the {metallicity, luminosity} relationship, even if we take into account the dilution effect just discussed for group R3. Merging scenarios must be envisaged for the formation of such objects.

The case of group R1 is even more challenging. We are dealing in this group with three among the four brightest cluster members (BCM). In a first approach, Mellier et al. (1988) identified two of them, nos. 20 and 35, as cD and D type galaxies, respectively. Considering the aperture size of the PUMA slit compared to the extension of the objects, it appears that we do not include much of the outer envelope in no. 20, whereas we analyze the entire bodies of nos. 35 and 1. This insures us of the homogeneity of the sampled system in the three objects building up group R1. Again

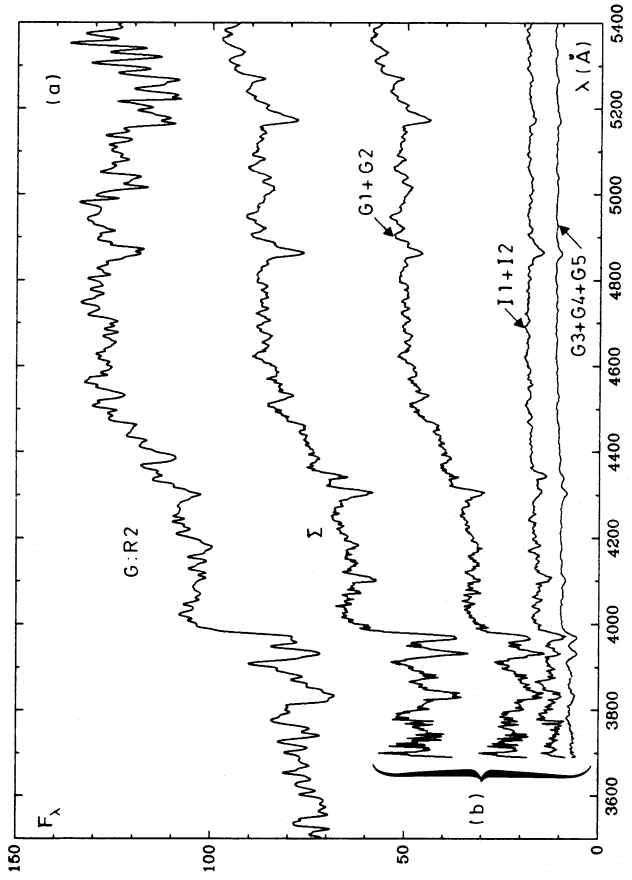

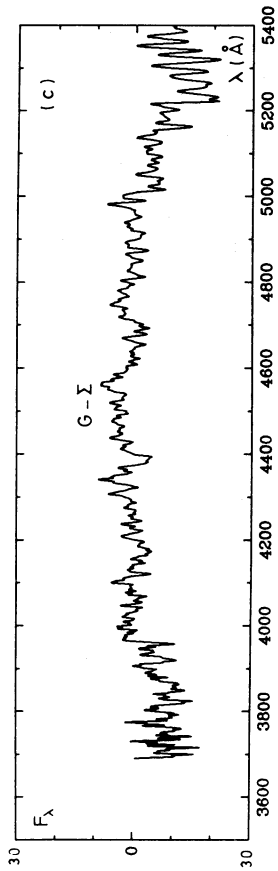

Fig. 4a–c. Same as Fig. 3 for group R2

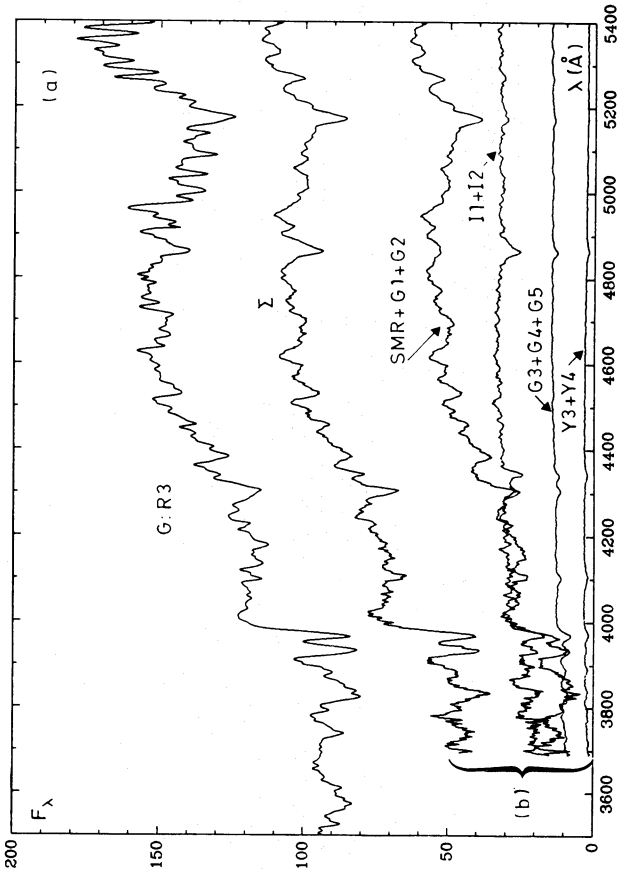

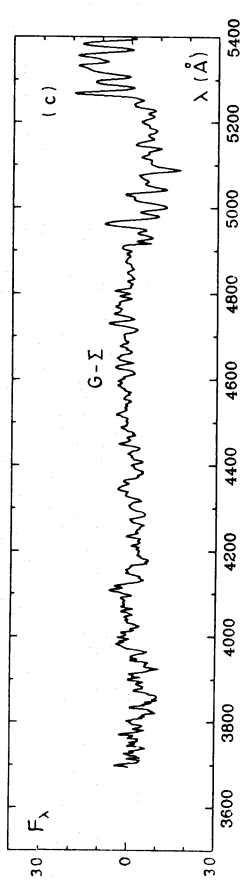

Fig. 5a–c. Same as Fig. 3 for group R3

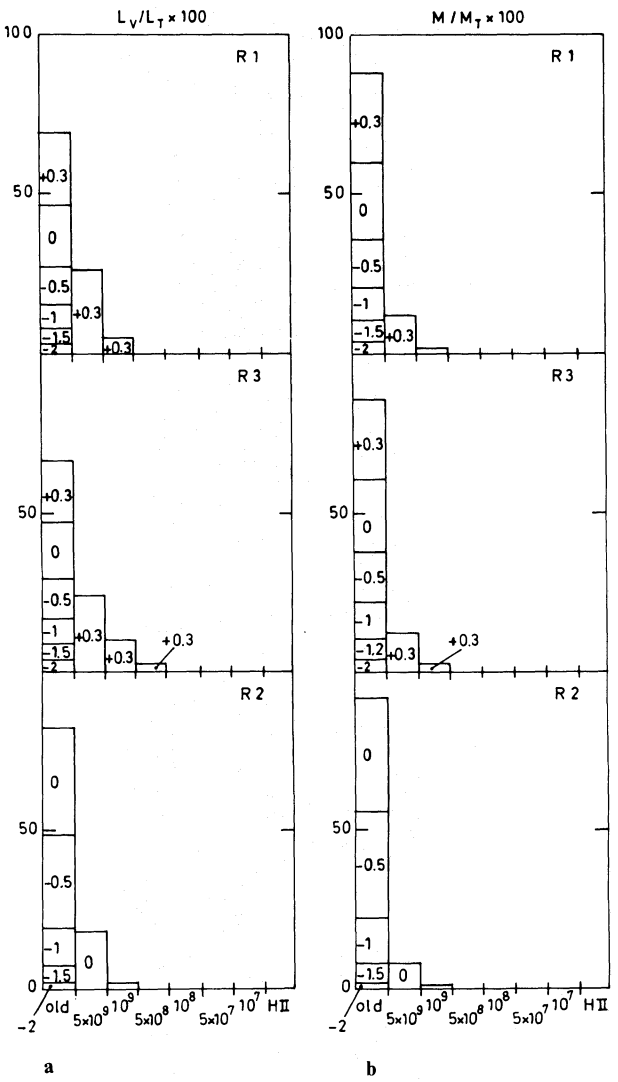

Fig. 6a and b. The V flux fractions (**a**) and mass fractions (**b**) from the different {age, metallicity} components for the three red groups R1 through R3. Metallicities $[Z/Z_\odot]$ are indicated (from -2 up to 0.6)

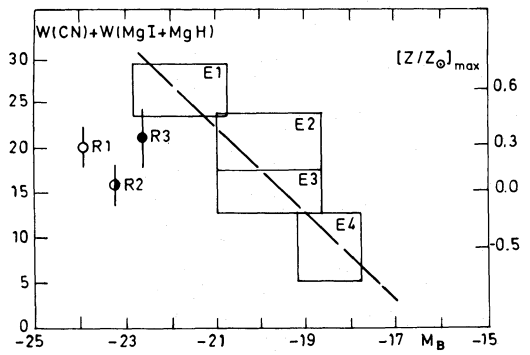

Fig. 7. The metallicity vs absolute blue magnitude relationship. The metallicity indicator is the sum W(CN 4150, 4214 Å) + W(Mg I, MgH, 5156, 5196 Å). The E1 through E4 boxes represent a decreasing luminosity sequence of elliptical galaxies after Bica (1988). The open circle represents group R1 in Abell 370, the semi-filled one corresponds to group R2 and the black-filled one to group R3. In the case of group R1, we have inferred the M_B value for one of its members (no. 1) from the R 24.5 mag

the low metallic content found for group R1 can be understood if the BCM arose from the merging of massive elliptical galaxies. The scenario is in agreement with the conclusions derived by Schombert (1987) following the original hypothesis of "galaxy cannibalism" by Ostriker and Tremaine (1975). It could explain as well the weaker Mg_2 gradient found in cD galaxies, with respect to that observed in elliptical galaxies (Gorgas et al., 1989).

Finally, our results argue for the merging process to have occurred *after* each of the merging components had already achieved the bulk of its star formation, hence of its chemical evolution. Else, the large amount of unprocessed gas collected through the merging should have led to a tremendous star formation rate and consequently to a large metal enrichment (extrapolating the metallicity vs luminosity relationship displayed in Fig. 7). The comparative analysis of groups R1 and R2 also suggests that the merging process is not only at work for building up cD objects, but is rather an on-going process among all bright elliptical galaxies in the core of galaxy clusters (Malumuth and Richstone, 1984; Merritt, 1984).

3.2.3. Results of the population synthesis for the blue groups B1 and B2

Results of the population synthesis for the two blue groups of galaxies are given in Table 3 and visualized in Figs. 8 through 11. The corresponding mass conversion is displayed in Figs. 12 and 13.

Regarding group B1, the best solution we could achieve consists of an approximately 50% flux contribution, at 5870 Å, from old populations with a maximum metal enrichment of up to $[Z/Z_\odot] = -0.5$. The rest of the light is due to a continuous, low level, star formation involving less than 15% of the galaxy mass. A late spiral type had been previously attributed by McLaren et al. (1987), to objects nos. 34 and 70 in group B1 while they did not observe no. 41. Two objects in group B1 were found also to be late spiral galaxies by Soucail et al. (1988), the third one being an irregular galaxy, according to a comparison with model synthetic spectra (Rocca-Volmerange and Guiderdoni, 1988). Because of the low level of continuous star formation we find, our population synthesis for group B1 roughly agrees with previous late spiral type assignments based upon the objects colours. In addition, the overall low metallicity we obtain suggests that the disc contribution is dominant over the bulge one. This again is compatible with this group being built from late spiral galaxies, as such morphological galaxy types have L(disc)/L(total) ~ 96% (Simien and de Vaucouleurs, 1986).

The case of group B2 did not appear as straightforward. Therefore, we tried several scenarios. The synthesis abbreviated B2c (Table 3, Fig. 9) represents the solution which we were first led to, without any constraint else than to follow a chemical evolutionary path. Notice that it exhibits a huge, old, metal-poor contribution which contradicts classical galaxy evolution theories. Because of the possible compensations already mentioned between age and metallicity effects when one deals with such a reduced spectral range and with blue populations, we decided to test other models.

In our first attempts, we modelized starbursts at intermediate (10^9, $5\,10^9$ yr) and young (10^8, $5\,10^8$ yr), ages, arbitrarily fixing their flux contribution at around 30%. All produce synthetic spectra similar to the one shown for the model abbreviated B2b

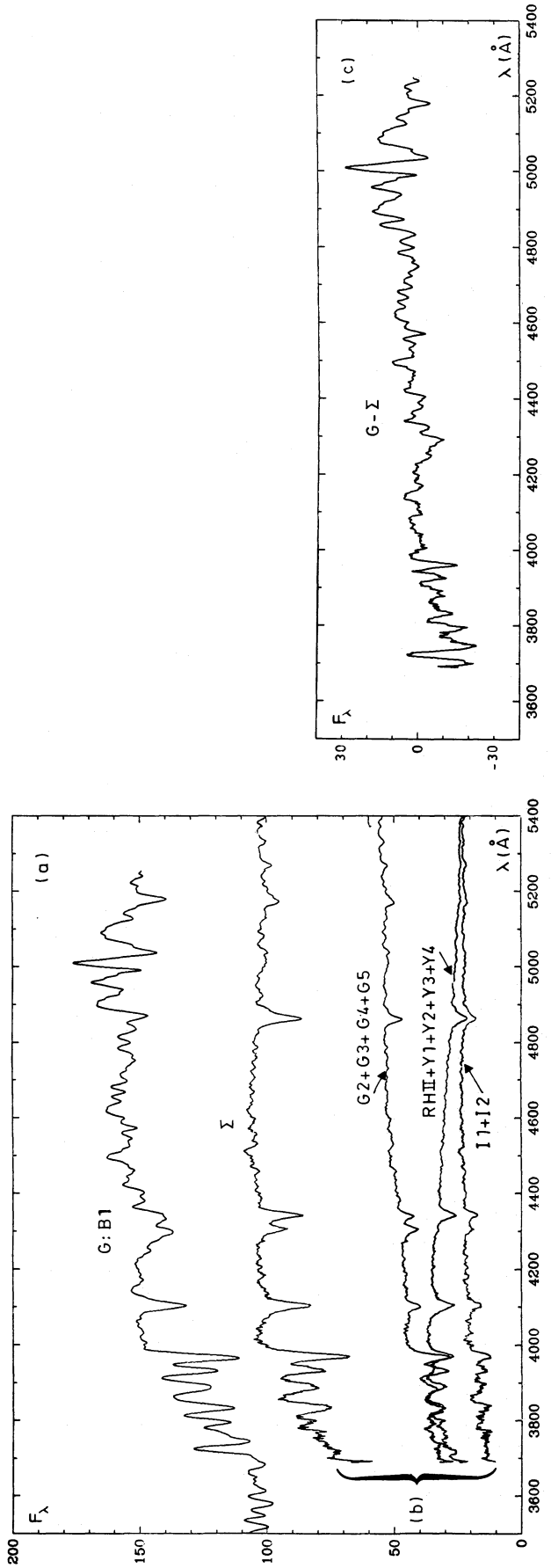

Fig. 8a–c. Same as Fig. 3 for group B1. Some smoothing was necessary as the stellar velocity dispersion was small with respect to the resolution we have in the cluster base

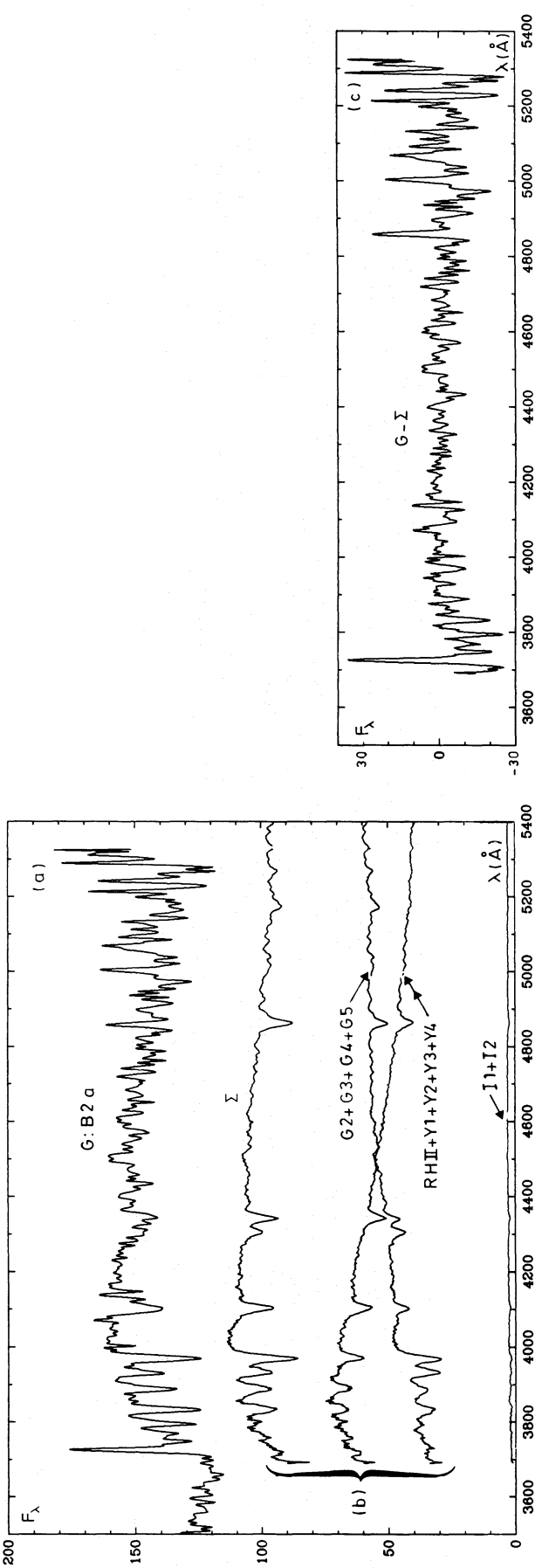

Fig. 9a–c. Same as Fig. 3 for group B2. Optimal solution B2a

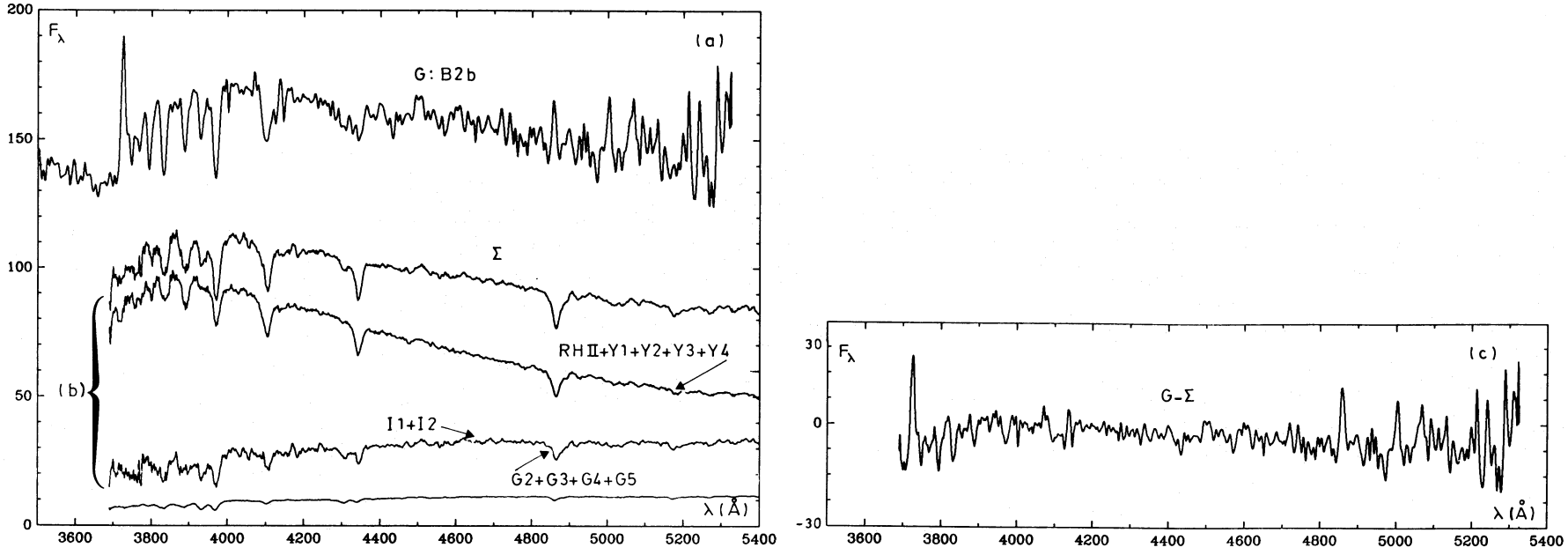

Fig. 10a–c. Same as Fig. 9. Attempt of a burst, B2b

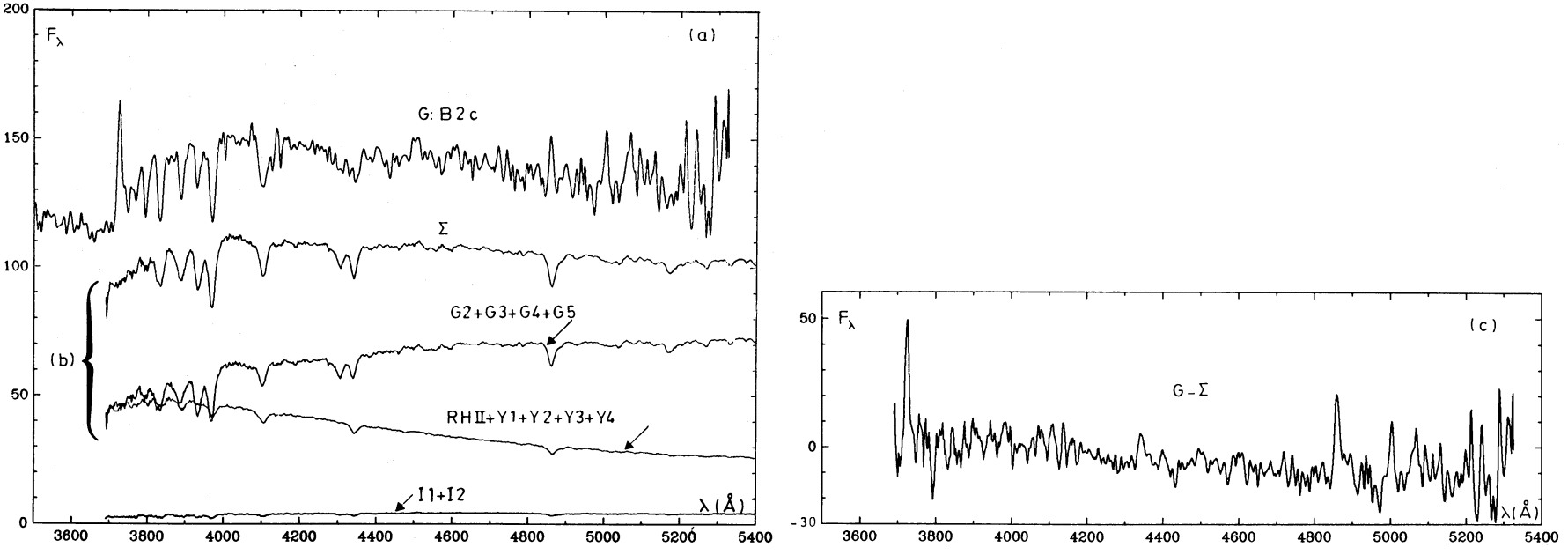

Fig. 11a–c. Same as Fig. 10. The "natural" model B2c

Table 3. Percentage flux contributions at 5870 Å, from the different {age, metallicity} components in the composite stellar populations of groups B1 and B2. B2a is the best solution. B2b and B2c correspond to alternative attempts (see Sect. 2.3). Same remark as in Table 2, regarding the table section labelled Test

H II	10^7	$5\,10^7$	10^8	$5\,10^8$	10^9	$5\,10^9$	Old	Age $[Z/Z_\odot]$	
3.2	4.2	4.4	4.0	5.9	9.4	13.4	16.	−0.5	
							15.4	−1	B1
{$E(B-V)=0.10$}							13.6	−1.5	
							10.5	−2	
15	9	5.6	5.3	2.2	1.5	1.4	15	−0.5	
							15	−1	B2a
{$E(B-V)=0$}							15	−1.5	
							15	−2	
21.4	14.2	8	7	3.7	2	32	2	−0.5	
							2.9	−1	B2b
{$E(B-V)=0$}							3.8	−1.5	
							3	−2	
13	5	2.5	2.5	1	1.5	2.5	11	−0.5	
							9	−1	
{$E(B-V)=0$}							15	−1.5	B2c
							37	−2	

Test features	Observed W_λ(Å); residue				
	B1	B2	a	b	c
Ca II K	6.8±1.0; −1.7	2.5±0.5;	−2.0	−1.7	−2.1
Hδ	4.8±1.2; +0.1	4.6±1.7;	+0.2	+0.6	+0.7
CN 4216	1.3±1.1; −2.1	0.1±1.2;	−1.9	−2.0	−1.6
CH Gband	5.6±0.3; +0.1	2.4±0.6;	−0.1	+0.2	−0.3
Hγ	6.0±1.0; −0.5	3.8±0.5;	+0.5	−0.8	−0.3
Hβ	3.6±0.7;	0.1±1.8;			
Mg I+MgH	3.0±1.8;	4.4±1.8;			

(Table 3, Fig. 10). A slight intrinsic reddening is then required in order to better match the observed continuum distribution. However, the ratios Ca II K/Ca II H+Hε and Hγ/Gb and are not well fitted. Further analyses led us to conclude that, for the type of evolutionary path we had selected, we could improve the fitting of Ca II K and Ca II H+Hε by attributing 15% *at least* of the total flux to the old, metal-poor component ($[Z/Z_\odot]=-2$). Then, the most plausible solution, consistent with chemical enrichment theories, was to fix every old component contribution at a comparable level (model labelled B2a in Table 3). No intrinsic reddening is required in that case. As shown in Table 3, an important flux contribution from very young components is then found in the synthesis. This agrees with the observed intense [O II] and [O III] emission lines. Although the synthesis result was strongly constrained for group B2, it indicates which way should be followed for understanding the star formation history in these objects. A more conclusive work could be achieved by extending the data wavelength range, particularly to the restframe ultraviolet.

4. Concluding remarks

1. In order to analyze in a quantitative way the composite stellar populations within galaxies of the distant cluster Abell 370 at redshift 0.374, we have had first to group objects with similar colors. The procedure resulted in a spectral data set with improved signal-to-noise ratio, although we evidently lost information about individual members. Five typical spectra were obtained, of which three relate to red galaxies R1 through R3 and two to blue galaxies B1 and B2. We have then proceeded with the stellar population analysis of the five groups.

2. We find that the three red objects are all consistent with being either giant elliptical galaxies (R3) or the result of galaxy merging processes (R1 and R2). The low metallicity found for R3 is explained through a dilution effect from the metal-poor halo component. In the case of R2 and R1, their low metallicity with respect to the standard metallicity versus absolute luminosity relationship, cannot be accounted for by this dilution effect only: it implies a merging process for the formation of these objects.

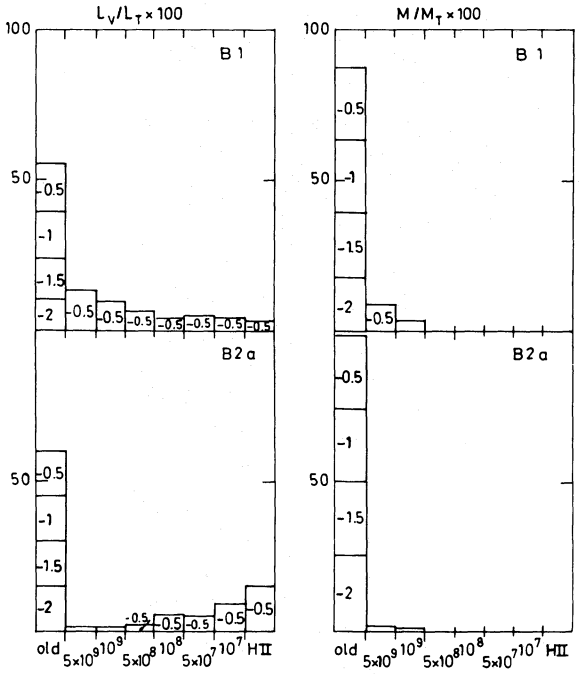

Fig. 12. Same as Fig. 6 for the best solutions of groups B1 and B2 (B2a)

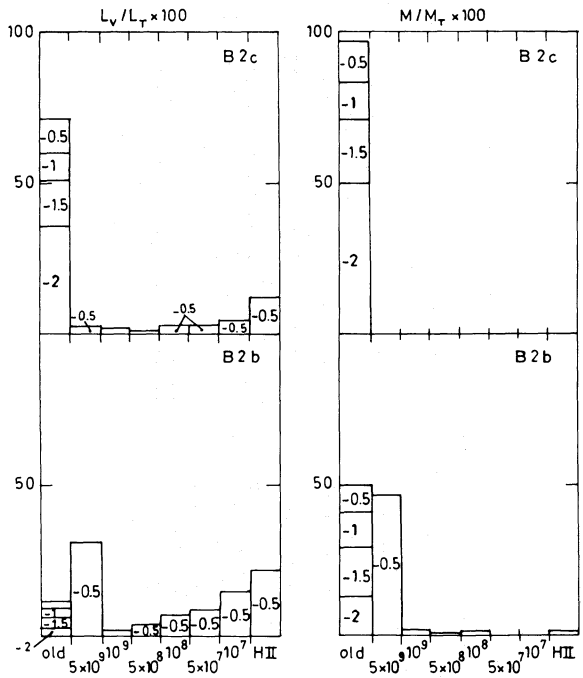

Fig. 13. Same as Fig. 6 for alternative, less performant solutions for group B2. (B2b and B2c)

The merging must have occurred well after the acting galaxies had achieved the bulk of their star formation and hence their chemical evolution. In no case do we find any trace of a cosmological evolution for the three groups of red galaxies in Abell 370 at $z = 0.374$.

3. The analysis of the two blue groups is limited by the restricted wavelength coverage of the available data. This limitation is more serious than for the red objects as, in blue populations, age and metallicity effects compete in the 3500–5500 Å region. However, a comparative synthesis of the two blue groups reveals that group B1 rather corresponds to conventional late spiral galaxies, while group B2 rather holds its blue colour from a recent burst of star formation, $5\,10^6$ yr old, involving an 0.1% mass fraction. Obviously this analysis would benefit from an extension of the wavelength coverage, and from the subsequent possibility to search through the entire (Z, age) plane, leaving aside the constraint of a chemical evolutionary path.

Acknowledgements. We are gratefully indebted to Y. Mellier and the whole group in Toulouse Observatory for providing a tape version of their spectral catalogue of galaxies in Abell 370.

References

Arimoto, N., Yoshii, Y.: 1987, *Astron. Astrophys.* **173**, 23
Bautz, M., Loh, E., Wilkinson, D.: 1982, *Astrophys. J.* **255**, 57
Bica, E.: 1988, *Astron. Astrophys.* **195**, 176
Bica, E., Alloin, D.: 1987, *Astron. Astrophys.* **181**, 270
Bica, E., Alloin, D.: 1988, in *Towards understanding galaxies at large redshifts*, eds. R. Kron, A. Renzini, Kluwer, p. 77
Bica, E., Arimoto, N., Alloin, D.: 1988, *Astron. Astrophys.* **202**, 8
Bothun, G., Dressler, A.: 1986, *Astrophys. J.* **301**, 57
Butcher, H., Oemler, A.: 1978, *Astrophys. J.* **219**, 18
Butcher, H., Oemler, A.: 1984, *Astrophys. J.* **285**, 426
Butcher, H., Oemler, A., Wells, D.: 1983, *Astrophys. J. Suppl. Ser.* **52**, 183
Coleman, G., Wu, C., Weedman, D.: 1980, *Astrophys. J. Suppl. Ser.* **43**, 393
Combes, F.: 1987, in *Starbursts and Galaxy Evolution*, eds. T.X. Thuan, T. Montmerle, J. Tran Thanh Van, Ed. Frontières, p. 325
Couch, W., Sharples, R.: 1987, *Monthly Notices Roy. Astron. Soc.* **229**, 423
Dressler, A.: 1986, in *Spectral evolution of galaxies*, eds. C. Chiosi, A. Renzini, Reidel, p. 375
Dressler, A., Gunn, J.: 1982, *Astrophys. J.* **263**, 533
Dressler, A., Gunn, J., Schneider, D.: 1985, *Astrophys. J.* **294**, 70
Ellis, R.: 1988, in *Towards understanding galaxies at large redshifts*, eds. R. Kron, A. Renzini, Kluwer, p. 147
Gorgas, J., Efstathiou, G., Aragon Salamanca, A.: 1987, *IAU Symp.* **127**, p. 189
Hartwick, F.: 1976, *Astrophys. J.* **209**, 418
Henry, J., Lavery, R.: 1987, *Astrophys. J.* **323**, 473
Koo, D.: 1988, in *Towards understanding galaxies at large redshifts*, eds. R. Kron, A. Renzini, Kluwer, p. 275
MacLaren, I., Ellis, R., Couch, W.: 1987, *Monthly Notices Roy. Astron. Soc.* **230**, 249
Malumuth, E.M.., Richstone, D.O: 1984, *Astrophys. J.* **276**, 413
Mellier, Y., Soucail, G., Fort, B., Mathez, G.: 1988, *Astron. Astrophys.* **199**, 13
Merritt, D.: 1984, *Astrophys. J.* **270**, 26
O'Connell, R.: 1988, in *Towards understanding galaxies at large redshifts*, eds. R. Kron, A. Renzini, Kluwer, p. 177
Ostriker, J.P., Tremaine, S.D.: 1975, *Astrophys. J.* **202**, L113

Pence, W.: 1979, *Astrophys. J.* **203**, 39
Persson, S.: 1988, in *Towards understanding galaxies at large redshifts*, eds. R. Kron, A. Renzini, Kluwer, p. 251
Pickles, A., van der Kruit, P.: 1988, in *Towards understanding galaxies at large redshifts*, eds. R. Kron, A. Renzini, Kluwer, p. 29
Rocca-Volmerange, B., Guiderdoni, B.: 1988, *Astron. Astrophys. Suppl. Ser.* **75**, 93
Schmidt, A., Bica, E., Alloin, D.: 1990, *Monthly Notices Roy. Astron. Soc.* **243**, 620
Schombert, J.M.: 1987, *Astrophys. J. Suppl. Ser.* **64**, 643
Sharples, R., Ellis, R., Couch, W., Gray, P.: 1985, *Monthly Notices Roy. Astron. Soc.* **212**, 687
Simien, F., de Vaucouleurs, G.: 1986, *Astrophys. J.* **302**, 564
Soucail, G., Mellier, Y., Fort, B., Cailloux, M.: 1988, *Astron. Astrophys. Suppl. Ser.* **73**, 471